

RNA denaturation: excluded volume, pseudoknots and transition scenarios

M. Baiesi,¹ E. Orlandini,¹ and A. L. Stella^{1,2}

¹*INFN-Dipartimento di Fisica, Università di Padova, I-35131 Padova, Italy.*

²*Sezione INFN, Università di Padova, I-35131 Padova, Italy.*

(Dated: September 8, 2018)

A lattice model of RNA denaturation which fully accounts for the excluded volume effects among nucleotides is proposed. A numerical study shows that interactions forming pseudoknots must be included in order to get a sharp continuous transition. Otherwise a smooth crossover occurs from the swollen linear polymer behavior to highly ramified, almost compact conformations with secondary structures. In the latter scenario, which is appropriate when these structures are much more stable than pseudoknot links, probability distributions for the lengths of both loops and main branches obey scaling with nonclassical exponents.

PACS numbers: 87.15.Aa, 87.14.Gg, 05.70.Fh, 64.60.Fr

In recent years, considerable attention has been devoted to the problem of describing the formation of secondary structure (base pairing map) in single molecular strands of RNA [1, 2, 3, 4, 5, 6, 7, 8]. The solution of such a problem is regarded as an important step within the general program of understanding how structure is encoded in the primary sequence of biopolymers. By making use of some simplifications, like that of disregarding excluded volume effects or pseudoknots formation, some studies established the existence of a molten phase at relatively high temperatures for an RNA molecule in dilute solution [9, 10, 11]. In this phase the inhomogeneities associated to a specific primary sequence should be irrelevant for the large scale behavior and should allow the coexistence of a very large number of different secondary structures of comparable free energy.

As the temperature T increases, a long RNA molecule should pass from the molten phase to a regime in which secondary structures essentially disappear and the global behavior becomes that of a linear polymer chain in good solvent. Excluded volume should play a relevant role at such a denaturation transition. Indeed, there the entropic free energy gain associated to the formation of hairpins or of more complicated branched structures with loops is comparable with the corresponding base pair binding and staking energies, and depends crucially on the repulsive interactions. Recent studies have shown that the discontinuous nature and the universal features of double stranded DNA denaturation are determined by excluded volume interactions [12, 13, 14].

To our knowledge, starting with the related pioneering work of de Gennes [15] on the statistics of branchings and hairpin helices in the periodic dAT copolymer, excluded volume effects were never fully taken into account in studies of RNA denaturation. This leaves open the problem of establishing the existence and of determining the possible character of this transition in the long chain limit. A realistic embedding of the system in space, taking into account excluded volume, is also a necessary condition for discussing pseudoknots and their consequences.

Pseudoknots occur, e.g., when two loops locally bind to each other determining a deviation of the configuration from planar topology [8]. Normally they are not included in models of the secondary structure [1, 2, 3, 5, 6, 16], or are considered as a perturbation [17].

In this Letter we propose a model of the large scale conformational behavior of RNA in the high T and molten phases. Although schematic, our model takes fully into account excluded volume and allows control of the effects of pseudoknots. While providing useful informations on the behavior of finite RNA chains, an extensive numerical analysis allows to draw precise scenarios for denaturation and the associated scaling regimes in different conditions.

At coarse-grained level we model a conformation of the RNA strand as a two-tolerant trail of N steps on the face centered cubic (FCC) lattice [26]. This is a random walk in which no more than two steps are allowed to overlap on a single lattice bond, forming what we call a contact. This restriction takes into account the excluded volume. In addition, by giving an orientation to the trail, we impose that only pairs of antiparallel steps can form contacts, and whenever this happens a gain in energy $\epsilon < 0$ is counted. The orientation of the trail reflects the backbone directionality or RNA [8]. In our model a contact corresponds to a sequence of bound base pairs over a distance of the order of the persistence length of the RNA double helix. This persistence length can vary with T near a denaturation transition. However, this effect should not matter for the large scale properties. Since our model is coarse-grained and we are not interested in T 's below those of the molten phase, we neglect also the heterogeneity of base pair interactions. Thus, ϵ represents an effective, average parameter.

Figure 1 reports schematically two possible configurations of our model. In both (a) and (b) a diagram on the right summarizes the corresponding contact map. A bridge in the diagrams connects each pair of steps forming a contact. Bridges are numbered in order of appearance if one follows the trail orientation. A main bridge is a bridge which is not inscribed within other, larger

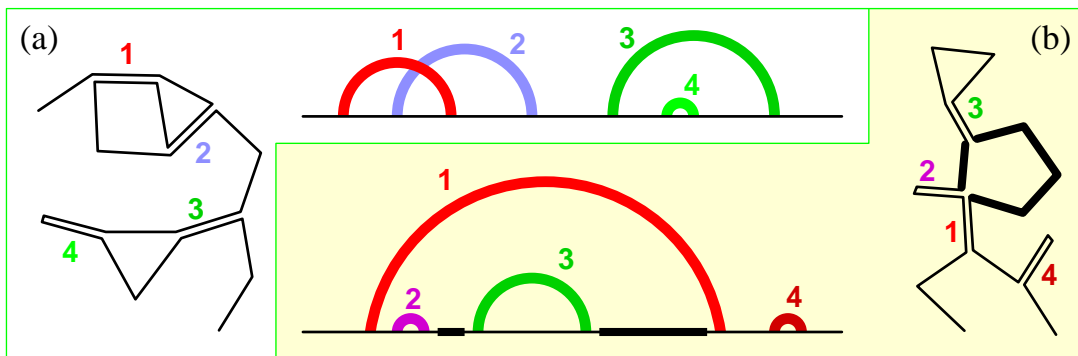


FIG. 1: RNA configurations and corresponding contact maps. Overlapped steps (contacts) are slightly split. In (a) a pseudoknot is present (crossing of bridge “1” with bridge “2”). In (b) a loop of length $\ell = 5$ is marked by a thicker line, both on the chain and in the contact map. Here, “1” and “4” are main bridges.

bridges. Unlike (b), (a) shows a pseudoknot, indicated by the crossing of two bridges in the diagram. This crossing means that a step forming a loop overlaps with one outside the loop. In order to investigate the role of pseudoknots, we consider two variants of the model, which we refer to as I and II. While in model I configurations with pseudoknots are allowed, in addition to those without pseudoknots, in model II the former are forbidden altogether. The choice of attributing the same energy to all kinds of contacts is a simplification of model I. Computationally it would be awkward to attribute selectively a weaker binding energy to those contacts which form pseudoknots, as physically appropriate in most situations [4].

Thermodynamic quantities and canonical averages are defined in terms of the partition function $Z = \sum_w \exp(-H(w)/T)$. The sum extends to all allowed configurations w with $|w| = N$ steps, and $H = \epsilon N_c(w)$, $N_c(w)$ being the number of contacts in w . For both models, we sampled configurations by a multiple Markov chain Monte Carlo procedure [18] using several (≈ 20) temperatures satisfying $0 \leq \epsilon/T \leq 3.5$ [27].

We first computed as a function of T the specific heat of model I and II for different N . At a continuous conformational transition with crossover exponent $\phi < 1$ one expects a singular behavior $C_{\max} \sim N^{2\phi-1}$ for the maximum of this quantity as $N \rightarrow \infty$ [19, 20]. In case $\phi < 1/2$ such singularity does not imply a divergence. For both models we find no evidence of a diverging C_{\max} . Hence, at this level we can only conclude that for both models the denaturation transition must be continuous and with $\phi < 1/2$, if it exists.

We also determined two geometrical radii of the configurations, namely the end-to-end distance, R_e , and the radius of gyration with respect to the center of mass, R_g . Multicritical phenomena theory [19, 21] has taught us that the ratios of the averages of such radii in the $N \rightarrow \infty$ limit are universal numbers characteristic of the different regimes involved in the transition. Fig. 2 shows

plots of $\langle R_e^2 \rangle / \langle R_g^2 \rangle$ for different N . For model I the trend of the curves gives indication of a sharp transition at $\epsilon/T \approx 1.9$. Indeed, for high T the ratio approaches from below the universal value 6.25(1) appropriate for a polymer in the swollen, self avoiding walk (SAW) regime [22]. On the other hand, at very low T 's the trail should fold in double structures with maximal number of contacts ($N_c \sim N/2$), in which R_e necessarily approaches zero. This explains the trend towards zero (from above) of the curves at low T . Remarkable is the accumulation of intersection points for $\epsilon/T \approx 1.9$. These intersections mark a change of the trend of the curves for increasing N and suggest the presence of a peculiar transition regime with universal ratio ≈ 4.8 . Hence, for model I there is clear evidence of a second order transition at $\epsilon/T \approx 1.9$. For model II there is no similar indication: the intersections are pushed towards lower and lower T 's as one

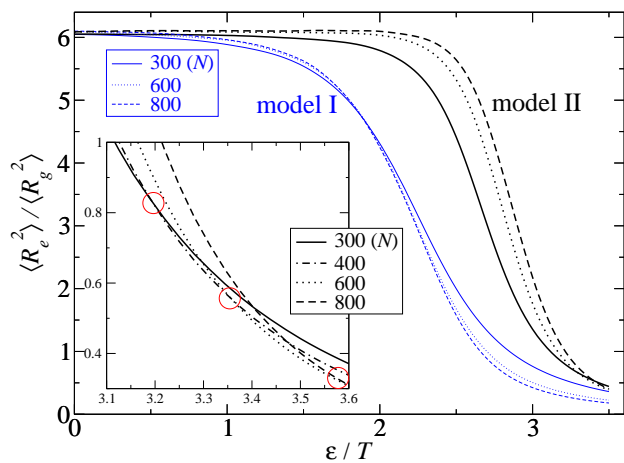


FIG. 2: $\langle R_e^2 \rangle / \langle R_g^2 \rangle$ as a function of ϵ/T for three different values of N . Inset: detail of the crossings of four curves for model II. The circles enclose intersections between the curve pairs (300, 400), (400, 600) and (600, 800).

compares curves corresponding to pairs of increasing N values (Fig. 2, inset). This means that the larger N , the deeper the SAW regime extends in the low T region. The whole pattern suggests for model II a smooth crossover, not a transition. Further insight is provided by the study of some scaling properties. The radius of gyration is expected to scale as $\langle R_g \rangle \sim N^\nu$ for large N [19]. For both models we observe that at high T the determinations of ν at finite N , for $N \rightarrow \infty$ approach a value ≈ 0.59 appropriate for a SAW in $d = 3$ [19, 22]. For model I, at T 's sufficiently below the transition the ν estimates can be extrapolated to ≈ 0.35 for large N . This indicates that the configurations are very close to compact in the low T , molten phase ($\nu \approx 1/d = 1/3$). For model II at very low T 's we extrapolate $\nu \approx 0.4$ which is also not far from $\nu = 1/2$, as expected for branched polymers [19], [28].

The different behaviors of the two models are due to the presence of pseudoknots in model I. Indeed, the fraction of sampled configurations with pseudoknots in model I is already substantial and increases with N at high T . It reaches soon values close to 1 near the transition and below. Pseudoknots correspond to the formation of extra binding contacts and thus can lead to more compact configurations with respect to the case of model II. These extra contacts trigger the sharp transition observed at $\epsilon/T \approx 1.9$. For model II, if present, a transition should be located at much lower T 's, most likely below the range of applicability of the model [29].

The possibility of forming pseudoknots is a driving factor in tertiary structure formation [4]. However, model I somehow overamplifies this factor, because it gives pseudoknot forming contacts an energy equal to that of the other contacts. In fact contacts forming pseudoknots should correspond most often to the weak binding of quite short portions of single strand loops, like for kissing hairpins. Longer bindings giving rise to pseudoknots are expected to be kinetically inhibited [5]. One way to make the energies of contacts forming pseudoknots closer to those of the other contacts is to introduce sufficiently high concentrations of divalent metal ions, like Mg^{2+} in solution [4, 23]. On the other hand, in model II pseudoknot forming contacts would appear if one would look at the details of the configurations at somewhat more coarse-grained level. This means that this model can be interpreted as one similar to model I, but giving essentially zero energy to such contacts. Thus, it is reasonable to expect the description of model II to be most appropriate for not too low T 's, and especially when, e.g., a low concentration of Mg^{2+} ions in solution enlarges the stability gap between secondary structure and pseudoknot forming links [4, 23].

RNA denaturation corresponds to a substantial suppression with increasing T of the highly ramified structure of loops and branches characterizing the molten phase. The analysis of the loops is feasible and particularly instructive in model II. For DNA, the distribution of

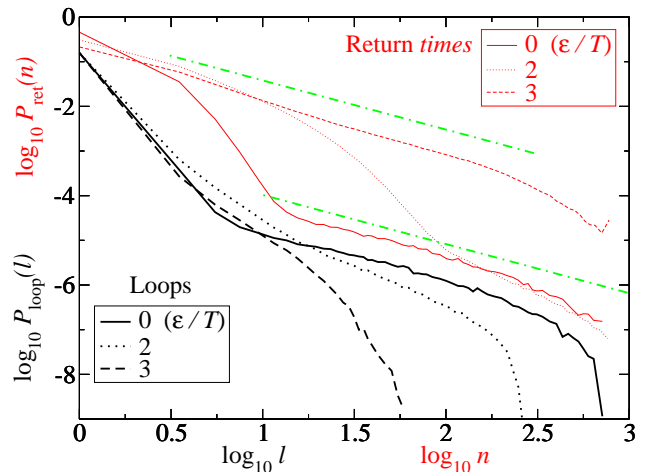


FIG. 3: Log-log plots for $P_{\text{loop}}(\ell)$ (thick lines, shifted down by 0.5 for clarity) and $P_{\text{ret}}(n)$ (thin lines, red online), both for $N = 800$ and for different T values. The dot-dashed lines have slope -1.1 .

the lengths of denaturated loops, corresponding to openings of the double helix, follows a power law whose exponent c determines the character of the transition [13, 14]. A simple example of loop in RNA is given by the closure of an isolated hairpin. In this case the loop is connected to the rest of the structure by a single branch of double steps in model II. Of course, more complicated situations may occur (thick loop in Fig. 1(b)). Even at high T an extensive number of minor spike-like branches is present along the RNA backbone. Thus, loops with a fixed number of branches naturally have length distributions with rather short cut-off. Therefore, we decided to sample the length of all loops identified in the various configurations, irrespective of the number of outgoing double step branches. The various lengths can be obtained from the contact map of each configuration, by using a recursive algorithm that identifies all the loops inside each main bridge in the diagram. Another interesting quantity is the return time, i.e. the total number of steps comprised within a main bridge. In the assumed planar topology of model II this time is the total arc length corresponding to each departure of the configuration from a contact-free, linear polymer behavior. Probability distributions of the loop lengths, ℓ , and of the return times, n , are plotted in Fig. 3 for different T 's and for $N = 800$. At high T , after transients both distributions behave as power laws with approximately identical exponents: $P_{\text{loop}}(\ell) \sim \ell^{-c_\ell}$, $P_{\text{ret}}(n) \sim n^{-c_r}$, with $c_\ell \simeq c_r = 1.1(1)$. The peaks at small ℓ and n in the distributions indicate that loops at high T mostly occur within isolated small hairpins in model II. The identity of c_ℓ and c_r means that almost all large bridges are also main bridges. Thus, the return time essentially coincides with the loop length at high T . At lower T , while P_{loop} becomes shorter and shorter ranged

for decreasing T , the behavior of P_{ret} remains of power law type at large arguments. The value of c_r remains stable and close to that estimated for $\epsilon/T = 0$. This means that as the RNA molecule enters deeper and deeper into the molten phase with developed secondary structures, the loops become shorter and shorter. On the other hand, the main branches departing from the contact-free backbone encompass all accessible length scales, as appropriate for a branched polymer. This could also explain why in this range of T the exponent ν discussed above is not far from $1/2$, as for branched polymers [19]. The exponent c_r obtained here definitely deviates from the mean field value $3/2$ [9].

Summarizing, for model I we could establish the existence of a sharp denaturation transition which is due to the presence of pseudoknots. Unlike the melting of DNA, this is a second order transition. Model I applies to experimental situations in which the stability gap between secondary and tertiary folding is sensibly reduced, e.g., by a high concentration of Mg^{2+} ions [4, 23]. On the other hand, one can regard model II as a more adequate description of RNA when the same stability gap is large, e.g. with low Mg^{2+} concentrations [4, 23]. In this model there is no sharp transition and the denaturation occurs as a crossover from linear to branched-compact polymer behavior. The geometry of this crossover is well described by the distributions P_{loop} and P_{ret} and by their exponents, whose nonclassical values are a further consequence of excluded volume.

We acknowledge discussions with E. Carlon. The work was supported by MIUR-COFIN01 and by INFM-PAIS02.

[1] M. Zuker, *Science* **244**, 48 (1989).
 [2] I. L. Hofacker et al., *Monatshefte für Chemie* **125**, 167 (1994), URL <http://www.tbi.univie.ac.at/~ivo/RNA>.
 [3] P. G. Higgs, *Phys. Rev. Lett.* **76**, 704 (1996).
 [4] I. Tinoco Jr. and C. Bustamante, *J. Mol. Biol.* **293**, 271 (1999).
 [5] R. Bundschuh and T. Hwa, *Phys. Rev. Lett.* **83**, 1479 (1999).
 [6] A. Pagnani, G. Parisi, and F. Ricci-Tersenghi, *Phys. Rev. Lett.* **84**, 2026 (2000).
 [7] S.-J. Chen and K. A. Dill, *Proc. Nat. Acad. Sci. USA* **97**,

646 (2000).
 [8] P. G. Higgs, *Quart. Rev. Biophys.* **33**, 199 (2000).
 [9] R. Bundschuh and T. Hwa, *Phys. Rev. E* **65**, 031903 (2002).
 [10] R. Bundschuh and T. Hwa, *Europhys. Lett.* **59**, 903 (2002).
 [11] M. Müller, *Phys. Rev. E* **67**, 021914 (2003).
 [12] M. S. Causo, B. Coluzzi, and P. Grassberger, *Phys. Rev. E* **62**, 3958 (2000).
 [13] Y. Kafri, D. Mukamel, and L. Peliti, *Phys. Rev. Lett.* **85**, 4988 (2000).
 [14] E. Carlon, E. Orlandini, and A. L. Stella, *Phys. Rev. Lett.* **88**, 198101 (2002).
 [15] P.-G. de Gennes, *Biopolymers* **6**, 715 (1968).
 [16] R. Nussinov and A. B. Jacobson, *Proc. Nat. Acad. Sci. USA* **77**, 6309 (1980).
 [17] H. Orland and A. Zee, *Nucl. Phys. B* **620**, 456 (2002).
 [18] M. C. Tesi, A. J. Janse van Rensburg, E. Orlandini, and S. G. Whittington, *J. Stat. Phys.* **29**, 2451 (1996).
 [19] C. Vanderzande, *Lattice models of Polymers* (Cambridge University Press, 1998).
 [20] E. Orlandini, F. Seno, and A. L. Stella, *Phys. Rev. Lett.* **84**, 294 (2000).
 [21] V. Privman, P. C. Hohenberg, and A. Aharony, in *Phase Transitions and Critical Phenomena*, edited by C. Domb and J. L. Lebowitz (Academic Press, New York, 1991), vol. 14, p. 1.
 [22] B. Li, N. Madras, and A. Sokal, *J. Stat. Phys.* **80**, 661 (1995).
 [23] V. K. Misra and D. E. Draper, *Biopolymers* **48**, 113 (1998).
 [24] A. M. Ferrenberg and R. H. Swendsen, *Phys. Rev. Lett.* **61**, 2635 (1988).
 [25] E. Orlandini, F. Seno, A. L. Stella, and C. Tesi, *Phys. Rev. Lett.* **68**, 488 (1992).
 [26] The FCC lattice allows for closed loops also of odd length and thus enriches their sampling.
 [27] To increase the mobility of the Markov chain at low T , where branched structures are expected, in addition to the usual set of local and pivot moves (see [18] and references therein), we implemented a variant of the pivot move, in which only one arm of the branched structure is rotated. In order to obtain smooth plots, data were processed by means of the multiple histogram method [24].
 [28] Two tolerant trails have been used to model collapse from SAW to branched polymer behavior [25]. See also P. Leoni and C. Vanderzande, to be published.
 [29] At low enough T the molten phase is supposed to leave place to a glassy one, in which the inhomogeneities due to primary structure become relevant [3, 5, 6, 9, 10].